Article

Not peer-reviewed version

Study of Anisotropy in High Temperature Tensile and Shear Deformation Behavior of Zirconium-2.5Nb Alloy and Evaluation of Parameters of Hill's Material Model

A. Syed and M.K. Samal *

Posted Date: 9 April 2026

doi: 10.20944/preprints202604.0659.v1

Keywords: Indian pressure tube material; Zr-2.5Nb alloy; anisotropy; stress-strain curve; Hill's plasticity model; orientation dependence; mechanical property; high temperature data

Article

Study of Anisotropy in High Temperature Tensile and Shear Deformation Behavior of Zirconium-2.5Nb Alloy and Evaluation of Parameters of Hill's Material Model

A. Syed [1,2] and M.K. Samal [1,2,*]

[1] Divison of Engineering Sciences, Homi Bhabha National Institute, Mumbai-400085, India
[2] Reactor Safety Division, Bhabha Atomic Research Centre, Trombay, Mumbai-400085, India
* Correspondence: mksamal@barc.gov.in or mksamal@yahoo.com; Tel.: +91-22-25593551; Fax: +91-22-25505151

Abstract

Pressure tubes (channels containing fuel in CANDU type nuclear reactors) of Indian pressurized heavy water reactors are made from quadruple-melted Zr-2.5Nb alloy. Owing to the texture and crystal structure, these tubes exhibit anisotropy in mechanical properties. During postulated severe accident scenario such as loss of coolant accident, the temperature of the pressure tube may rise rapidly due to disruption in the heat removal porcess from the fuel bundles. The deformation behavior of the pressure tube under such high temperature shall effect the integrity of the coolant channel. Hence, it is crucial to model the high temperature deformation behavior of pressure tube under these conditions. For design and safety analysis of pressure tube, the high temperature properties are required. In this work, tensile tests were carried out using the specimens cut from quadruple melted Zr2.5%Nb pressure tube along longitudinal, transverse and radial directions at temperatures, i.e., from 25˚C to 800˚C. Shear properties were also evaluated by using the specimen machined from longitudinal-circumferential orientation of tube. It was observed that the specimen oriented along the circumferential direction has highest strength, while the radial specimen has the lowest strength as compared to other direction specimens at all temperature conditions. With the increase in temperature above 600^{o}C, the material undergoes superplastic deformation with strain values reaches above 400% at 800^{o}C. In addition, an algorithm has been developed to determine the anisotropic parameters of Hill's yield function as a function of temperature and equivalent plastic strain using the experimental data. The equivalent stress-strain curves considering anisotropy have also been evaluated as a function of temperature. These data shall be useful for design and safety analysis of the pressure tube for different types of postulated loading and accidental conditions.

Keywords: Indian pressure tube material; Zr-2.5Nb alloy; anisotropy; stress-strain curve; Hill's plasticity model; orientation dependence; mechanical property; high temperature data

1. Introduction

Zr2.5Nb alloy pressure tubes (PT) are used as pressure boundary for the hot heavy water coolant in Indian Pressurized Heavy Water Reactors (PHWRs) due to their low neutron absorption, good resistance to corrosion and excellent material properties at reactor operating temperature of about 300ºC. During severe accident scenario such as loss of coolant accident (LOCA), the coolant may gets boiled off leading to degradation in heat transfer to the coolant. This causes significant increase in temperature of the PT above its operating temperature leading to its ballooning deformation. This radial deformation causes the contact between the PT and calandria tubes (CT). It is important to study the deformation of the pressure tube at high temperature as it controls how the heat shall be dissipated to the moderator which as a sink during an accident scenario.

 doi:10.20944/preprints202604.0659.v1

Pressure tubes are manufactured by two stage of hot extrusion of quadruple vacuum arc-melted Zr2.5Nb ingots. This is followed by two stage of cold pilgering with an intermediate annealing leading to final dimensions of the tube. During fabrication of the tubes, a two phase microstructre with strongly textured and elongated α-grains along the axial direction gets developed. Majority of the basal poles of α-grains gets aligned along the transverse direction that increases the strength of tube along this direction. The HCP structure of α-grains combined with mechanical working causes the anisotropy in mechanical properties of PT.

In recent research literature [1–10], the results of several studies on deformation, hydriding and creep behavior of Zr2.5Nb pressure tube material have been presented. The in-reactor deformation of cold-worked Zr2.5Nb pressure tubes were studied by Holt [1]. Apart from reactor applications, these alloys are also used in medical implant applications due to their superior strength, corrosion and waer resstance properties. In Ref. [2], the corrosion and wear resistance properties of medical implant grade Zr-2.5Nb alloy were studied and the effect of thermal oxidation treatment on these properties were considered. The corrosion behavior and wear resistance properties of these alloys as obtained after thermal oxy-nitriding treatment were also studied in Ref. [3], where these alloys were studied for their potential applications as coatings of industrial components. The impact of hydrides on the fracture toughness and the effect of temperature on the delayed hydride cracking rate of Zr-2.5Nb alloy were also studied in Refs. [4–6]. The performance of pre-oxidation films on Zr-2.5Nb pressure tube for preventing further corrosion in the reactor during operation was studied in Ref. [7]. Some high temperature tests on Zr2.5Nb alloy were conducted in Ref. [8]. Fatigue crack initiation models considering axial flaws in the pressure tube were presented in Ref. [9]. The anisotropy in mechanical properties, plastic flow and hardening behavior of these alloys for a limited range of temperatures (25-300^{o}C) were presented in Refs. [10–14]. The effects of microstructural variations as obtained from various manufacturing processes and its effect on mechanical properties were studied in Refs. [15–18]. The effects of crystallographic texture on anisotropic behavior of thermal expansion of this alloy were studied in Ref. [19]. The data on crack propagation in Zr2.5Nb alloy and the fracture toughness behavior were presented in Refs. [20–22]. The creep deformation behavior of the alloy were studied in Refs. [23,24]. From a comprehensive review of literature on different studies for this alloy, it was observed that the very high temperature data concerning the tensile and shear deformation of Zr2.5Nb alloy is not available in literature and hence, the objective of the current work to address this gap.

During severe accident scenario such as LOCA, the temperature of the pressure tube may rise rapidly due to disruption in heat removal from the fuel bundles. The deformation behavior of the pressure tube under high temperature shall effect the integrity of coolant channel. Hence, it is crucial to determine how the pressure tube will behave under these conditions that will control the dissipation of core heat to the surrounding moderator. The material properties of pressure tube along different orienations (i.e., longitudinal, trasnverse and radial) has not been studied previously in great details and its temperature dependence is another area which needs to be investigated systematically. Also, a procedure to estimate the anisotropic flow parameters of Hill's yield function are discussed in this paper.

In this work, tensile tests were carried out using the specimens cut from quadruple melted Zr2.5Nb pressure tube along longitudinal, transverse and radial directions at temperatures upto 800°C. Shear properties were also evaluated by using the specimen machined from longitudinal-transverse plane. An algorithm has been developed to determine the anisotropic parameters of Hill's yield function as a function of temperature and equivalent plastic strain using the experimental data.

The paper has been divided into six sections. In Section 2, the experimental procedure to evaluate tensile and shear properties of Zr2.5Nb alloy at different temperatures were presented. The results from the extensive experimental program were presented in Section 3. In Section 4, the engineering stress-strain curves of Zr2.5Nb alloy for different orientations and different temperatures were compared. The procedure for evaluation of anisotropic factors of the generalized Hill's yield model were presented in Section 5, followed by presentation of the results as obtained from the

Preprints.org (www.preprints.org) | NOT PEER-REVIEWED | Posted: 9 April 2026 doi:10.20944/preprints202604.0659.v1

calibration procedure. Some of the important conclusions from this work were presented in Section 6.

2. Experiments to Evaluate Tensile and Shear Properties of Zr2.5Nb Alloy at Different Temperatures

Specimens were cut from as received Zr2.5Nb pressure tubes of 550 MWe Indian PHWR. The inner diameter and thickness of PT taken for the study is around 103.4 mm and 4.5 mm respectively. Small specimens were designed and cut from the cylindrical tube such that no flattening of the tube shall be carried out. This was done to prevent any additional stresses due to flattening of the tube. Also, the design and fabrication of radial specimen is innovatively carried out. The details of the specimen design and other related discussions can be found in detail in Ref. [11]. The radial specimen was obtained from small thickness of PT of around 4.5 mm that has been a challenge. Shear specimen were also manufactured along longitudinal-transverse plane of the pressure tube. The shear specimen were designed such that pure shear loading should occur at the gauge region of the specimen. Shear specimens were cut from the tube along its circumference and same process is repeated for obtaining large number of shear specimens. These specimens were tested under tensile and shear loading to evaluate the effect of anisotropy on the material properties of the pressure tube.

The values of the anisotropic parameters (F, G, H and L) in the generalized Hill's anisotropic yield function have been evaluated from the tensile and shear experimental data. Tests have been carried out at temperature range of 25 to 800˚C as listed in **Table 1**. Tests were carried out in quasi-static loading conditions using displacement control loading mode with strain rate of around 5.5×10^{-4}/s. In order to ensure that the state of pure shear is attained at the gauge region of the shear specimen, a 3D elastic-plastic finite element (FE) analysis has been carried out and the results are presented in Figure 1. The details of FE analysis can be found in Ref. [11]. The results of engineering stress-strain curve of the specimen as obtained from FE analysis is shown in **Figure 1**, which corresponds to the shear stress-strain curve. The engineering stress-strain curve corresponding to tensile property of longitudinal specimen at room temperature is also shown in Figure 1 which is used as input in the FE analysis. It can be observed that the shear yield stress is 380 MPa, which is approximately 0.577 times the tensile yield stress value of the material, i.e., 650 MPa. Hence, this specimen is able to able to produce a state of stress corresponding to pure shear and it has been used for further tests to evaluate shear properties of pressure tube material in the longitudinal-transverse plane.

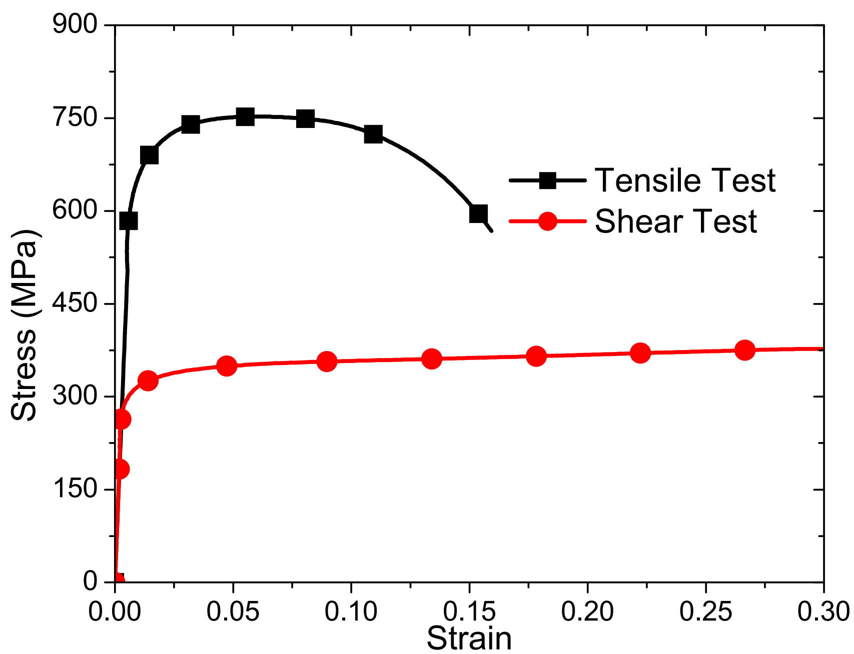

doi:10.20944/preprints202604.0659.v1

Figure 1. **Comparison of stress-strain curve as obtained from FE analysis for tensile and shear modes.**

Table 1. **Test matrix for tensile and shear testing of Zr-2.5Nb specimens of different orientations.**

Type of Test	Test No.	Specimen orientation	Temperature of Test (˚C)
Tensile	1	Longitudinal, transverse and radial specimens	25 (RT)
	2		100
	3		200
	4		300
	5		400
	6		500
	7		600
	8		700
	9		800
Shear	10	Shear	25 (RT)
	11	Shear	100
	12	Shear	200
	13	Shear	300
	14	Shear	400
	15	Shear	500
	16	Shear	600
	17	Shear	700
	18	Shear	800

3. Results from Experiments

3.1. Results of Tensile Tests for Specimens Oriented Along Transverse Direction

Specimens were machined from the transverse direction of the pressure tube as discussed earlier. Large number of tests have been carried out with the specimens oriented along the transverse direction in the temperature range of 25 to 800˚C. The picture of the experimental setup is presented in **Figure 2**. A number of tests have been carried out at the same temperature to check the repeatability of the tensile data. It can be observed from **Figure 3** that there is a good repeatability of the engineering stress-strain curve of the specimens as obtained from tests carried out at different test temperatures, ranging from 25^{o}C to 800^{o}C.

Preprints.org (www.preprints.org) | NOT PEER-REVIEWED | Posted: 9 April 2026 doi:10.20944/preprints202604.0659.v1

Figure 2. Specimen loaded in a furnace in the universal testing machine.

Figure 3(a) shows the engineering stress-strain curve for the specimen oriented along the transverse direction and tested at room temperature. The values of stress at which material yields along the transverse direction at room temperature (25˚C) were found to be 786 and 794 MPa respectively for test nos. 1 and 2 respectively. The values of ultimate tensile strengths of the specimens oriented along the transverse direction were found to be 842 and 858 MPa for test nos. 1 and 2 respectively. The value of ductility at failure of the specimens is measured to be around 14% for the transverse orientation.

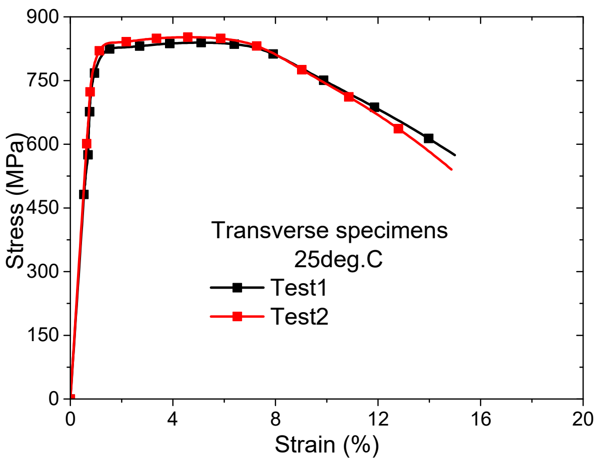

(a)

 doi:10.20944/preprints202604.0659.v1

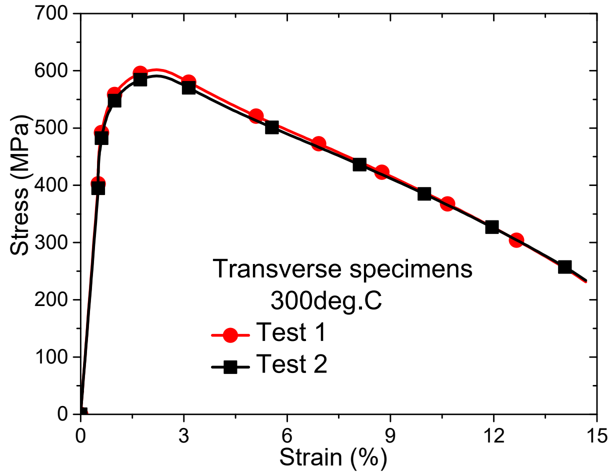

(b)

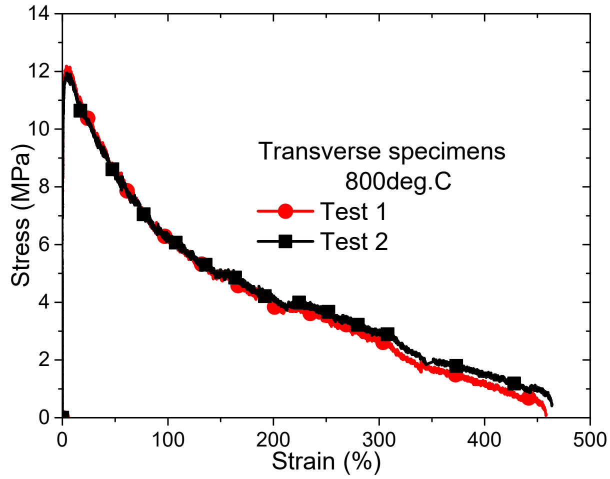

(c)

Figure 3. Engineering stress-strain curve of Zr2.5%Nb pressure tube material at two different temperatures and for transverse orientation. Repeatability of data for tests conducted as (a) 25°C; (b) 300°C; and (c) 800°C.

Figure 3(b) shows the engineering stress-strain curve for the transverse specimen tested at 300˚C. Yield strength of the material for the transverse orientation is 547 and 553 MPa for test nos. 1 and 2 respectively at 300˚C. The ultimate tensile strength for the transverse orientation is evaluated to be 594 and 606 MPa for test nos. 1 and 2 respectively at 300˚C. The ductility values of the specimens are 15% approximately.

Figure 3(c) shows the engineering stress-strain curve for the transverse specimen tested at 800˚C. Yield strength of the material for the transverse orientation is 11.1 and 11.9 MPa for test nos. 1 and 2 respectively at 800˚C. The ultimate tensile strength for the transverse orientation is evaluated to be 12.2 and 12.8 MPa for test nos. 1 and 2 respectively at 800˚C. The ductility values of the specimens are 470% approximately.

The average values of yield strength, ultimate tensile strength and ductility values for the transverse orientation of the pressure tube at different temperatures are listed in **Table 2**. A comparison of the photographs of the specimens tested at different temperature can be seen from **Figure 4**. It can be seen that there is large increase in the specimen length after testing at 800˚C due to the superplastic nature of high temperature deformation behavior of Zr2.5Nb above 650˚C.

Table 2. Summary of mechanical properties of Zr2.5Nb alloy for transverse orientation.

Temperature (˚C)	Avg. Yield strength (MPa)	Avg. Ultimate tensile strength (MPa)	Avg. Ductility (%)
RT (25)	790	850	14.5
100	660	770	15.5
200	590	650	16
300	550	600	15
400	490	550	21
500	325	350	45
600	106	125	84
700	32	36	350
800	11.5	12.5	470

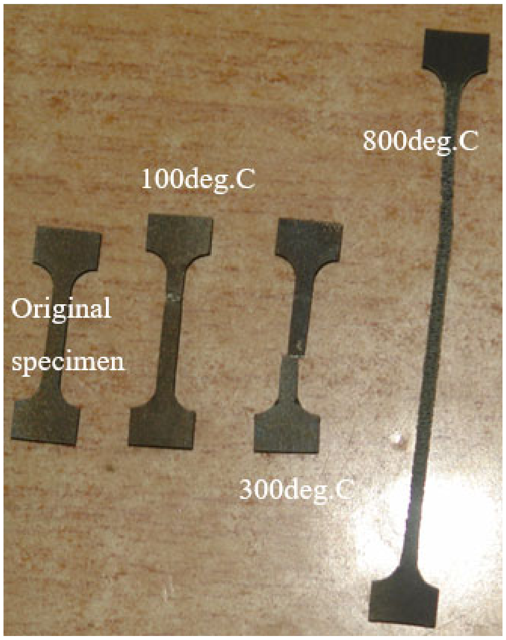

Figure 4. Comparison of transverse specimen tested at different temperature.

 doi:10.20944/preprints202604.0659.v1

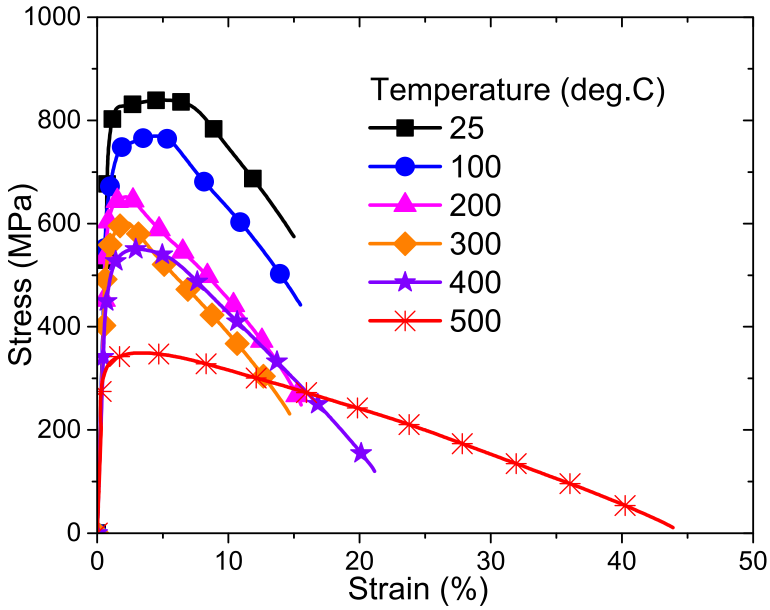

(**a**)

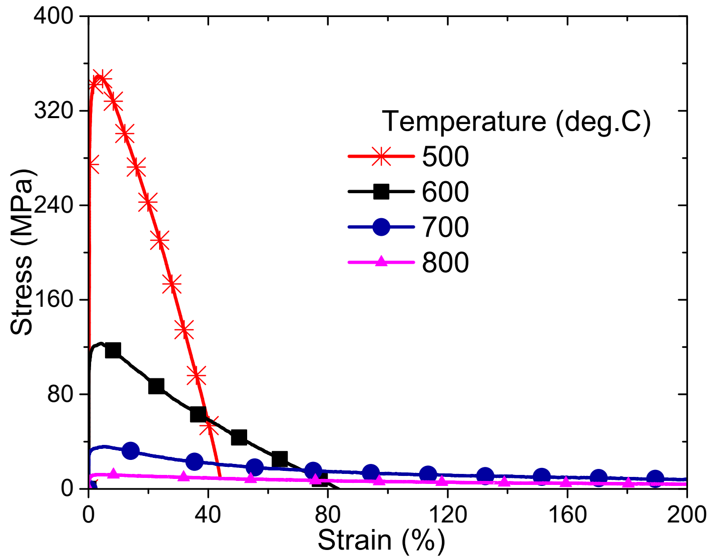

(**b**)

Figure 5. Variation of average stress-strain curve along the transverse orientation of the Zr2.5%Nb pressure tube with temperature (a) upto 500˚C (b) 500–800˚C.

The variation of average stress-strain curve along the transverse orientation of the pressure tube with temperature is shown in **Figure 5**. It can be observed that with the increase in temperature, there is a reduction in the value of yield strength and ultimate tensile strength, whereas, the average value of ductility increases with temperature. It was observed that there is not much change in ductility of specimens tested below 300˚C. Hardening of the transverse specimen is observed at test temperature of 25 and 100˚C. After 100˚C, hardening gets reduces and the material starts to soften as it reaches the ultimate tensile strength of the material. There is sharp reduction in strength of PT material above 600˚C with simultaneous increase in ductility. After 600˚C, it was observed the material undergoes superplastic deformation and the ductility values increases above 400%.

3.2. Results of Tensile Tests for Specimens Oriented Along Longitudinal Orientation

Several tests have been carried out at different temperatures for evaluating the material stress-strain behavior of pressure tube material in longitudinal direction. Average YS and UTS of the

 doi:10.20944/preprints202604.0659.v1

material in longitudinal direction tested at room temperature have been evaluated to be 650 and 750 MPa respectively. The same at 300˚C comes out to be 480 and 570 MPa respectively. Similarly, for the specimen tested at 600˚C, YS and UTS are 88 and 105 MPa respectively while the YS and UTS get reduced to 10.5 and 11.5 MPa respectively with the increase in temperature to 800˚C. Comparison of the stress-strain curve at different temperatures is shown in **Figure 6**. It can also be observed that the ductility of the material gets increased with the increase in temperature from RT to 800˚C. Ductility of the longitudinal specimen is found out to be 15.5, 18, 95 and 480% respectively for the specimens tested at RT, 300, 600 and 800˚C respectively. Final details of the results (i.e., average values) obtained from testing of specimens oriented along transverse direction of pressure tube are listed in **Table 3**.

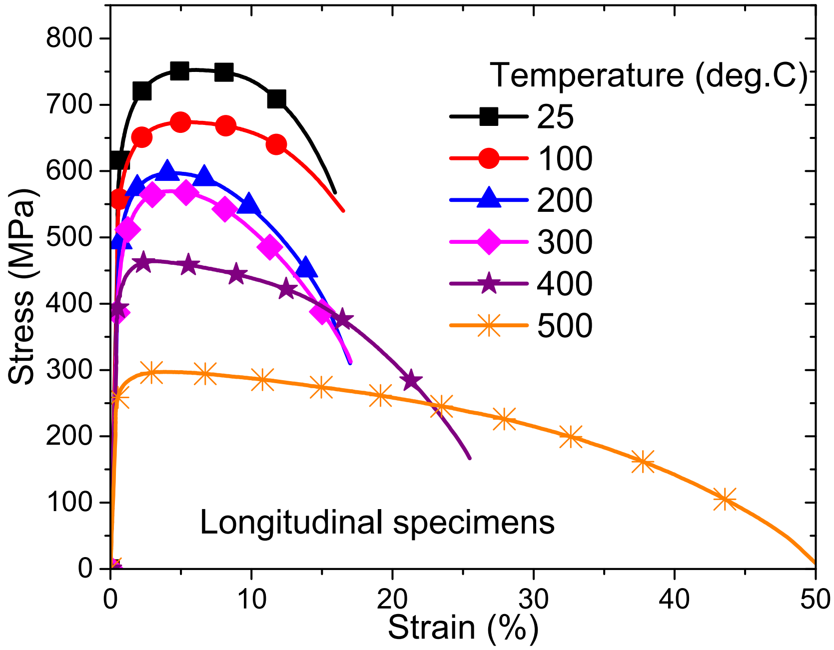

(**a**)

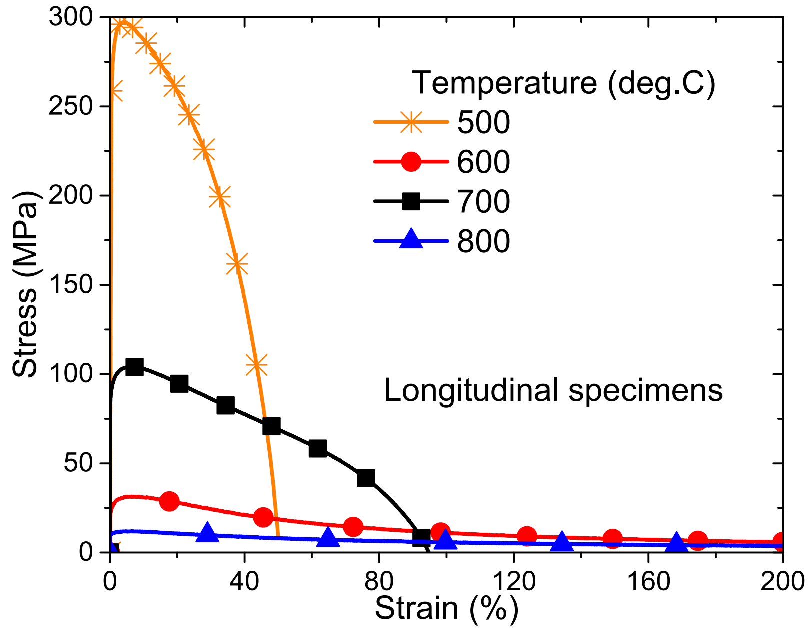

(**b**)

Figure 6. Comparison of stress-strain curve of Zr-2.5% Nb for transverse specimens at different temperatures (a) upto 500˚C (b) 500–800˚C.

Table 3. Summary of mechanical properties of Zr-2.5Nb alloy for longitudinal orientation.

Temperature (˚C)	Avg. Yield strength (MPa)	Avg. Ultimate tensile strength (MPa)	Avg. Ductility (%)
RT (25)	650	750	15.5
100	580	675	16.5
200	520	600	17
300	480	570	18
400	425	465	26
500	275	300	50
600	88	105	95
700	29	32	400
800	10.5	11.5	480

3.3. Results of Tensile Tests for Specimens Oriented Along Radial Orientation

Large number of tests have been carried out at different temperatures for evaluating the material stress-strain behavior of pressure tube material in the range of RT to 800°C. Average values of YS and UTS of the material from the radial specimens tested at room temperature have been evaluated as 550 and 630 MPa respectively. YS and UTS at 300°C are evaluated as 450 and 500 MPa respectively. Similarly, for the specimen tested at 600°C, YS and UTS have been evaluated as 65 and 77 MPa respectively while the YS and UTS get reduced to 10 and 10.5 MPa respectively with the increase in temperature to 800°C. Comparison of the stress-strain curve at different temperatures is shown in **Figure 7**. It can also be observed that, like longitudinal and transverse directions, the ductility of the material, in radial direction, gets increased with the increase in temperature from RT to 800°C. Ductility of the radial specimen is found to be 30, 65, 285 and 660% respectively for the specimen tested at RT, 300, 600 and 800°C respectively. Final summary of the test result for the radial specimens is listed in **Table 4**.

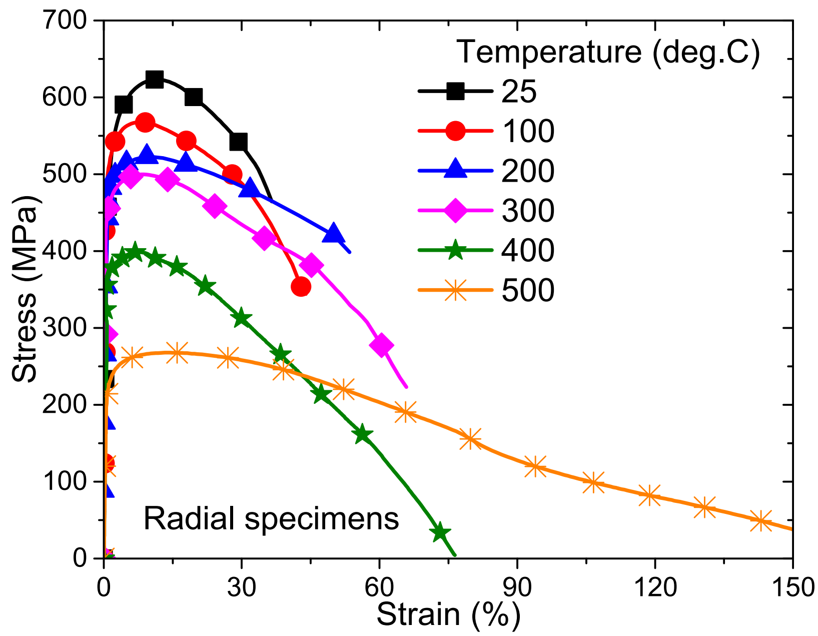

(a)

 doi:10.20944/preprints202604.0659.v1

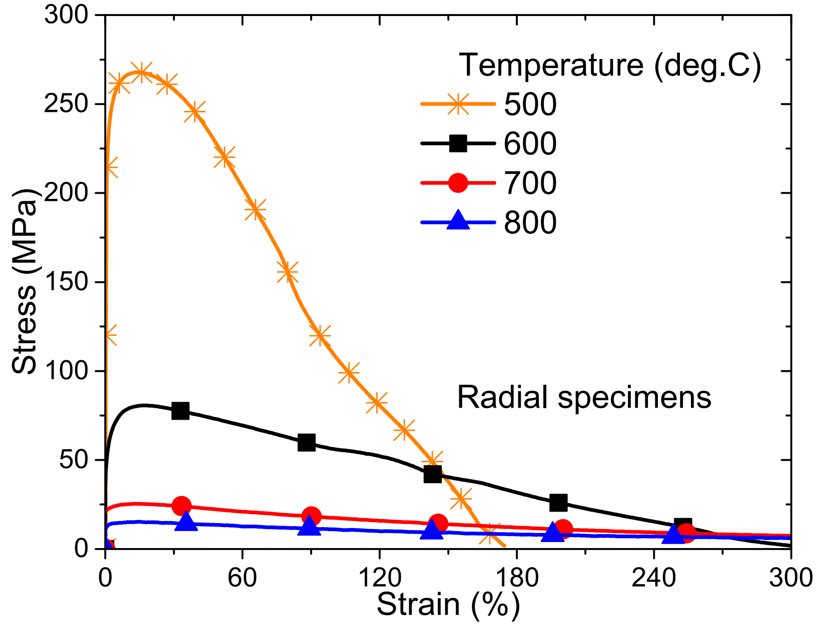

(b)

Figure 7. Comparison of stress-strain curve of Zr-2.5% Nb for radial specimens at different temperatures (a) upto 500˚C (b) 500–800˚C.

Table 4. Summary of mechanical properties of Zr-2.5Nb alloy for radial orientation.

Temperature (˚C)	Avg. Yield strength (MPa)	Avg. Ultimate tensile strength (MPa)	Avg. Ductility (%)
RT (25)	550	630	30
100	510	570	44
200	480	525	54
300	450	500	65
400	360	400	75
500	215	270	175
600	65	77	285
700	19	22	670
800	10	10.5	660

3.4. Results of Shear Tests for Specimens in Longitudinal-Transverse Plane

Several tests have been carried out at different temperatures for evaluating the shear stress-strain curve of pressure tube material in the longitudinal-transverse plane in the range of 25 to 800^{o}C. The photographs of the shear specimen before and after the tests are presented in **Figure 8**.

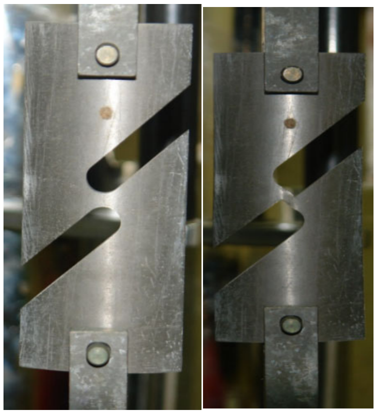

(a) (b)

Figure 8. Shear specimen loaded on the machine using the attachments and pins (a) specimen before application of load (b) specimen just before fracture.

It can be observed that the state of stress at the central gage region of the specimen corresponds to that of pure shear as the specimen is loaded along the longitudinal direction. Shear yield strength and maximum shear strength of the shear specimen tested at room temperature have been evaluated as 300 and 396 MPa respectively. Shear yield strength and maximum shear strength at 300°C were found to be 198 and 270 MPa respectively. Similarly, for the specimen tested at 600°C, shear yield strength and maximum shear strength have been evaluated as 42 and 62.4 MPa respectively while the corresponding values are 5.4 and 6.9 MPa respectively with the increase in temperature to 800°C. Comparison of the shear stress-strain curves at different temperatures is shown in **Figure 9**. It can also be observed that the shear ductility of the material in the longitudinal-transverse plane gets increased with the increase in temperature from 25 to 800°C. Shear ductility values of the specimens are found out to be 40, 115, 400 and 760% respectively for the specimens tested at 25, 300, 600 and 800°C. The summary of the test results for the shear type of specimens is presented in **Table 5**.

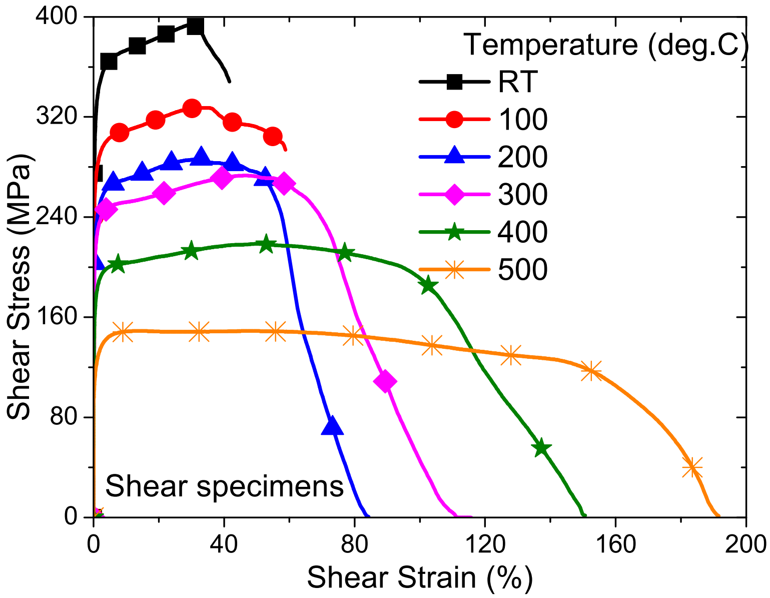

(a)

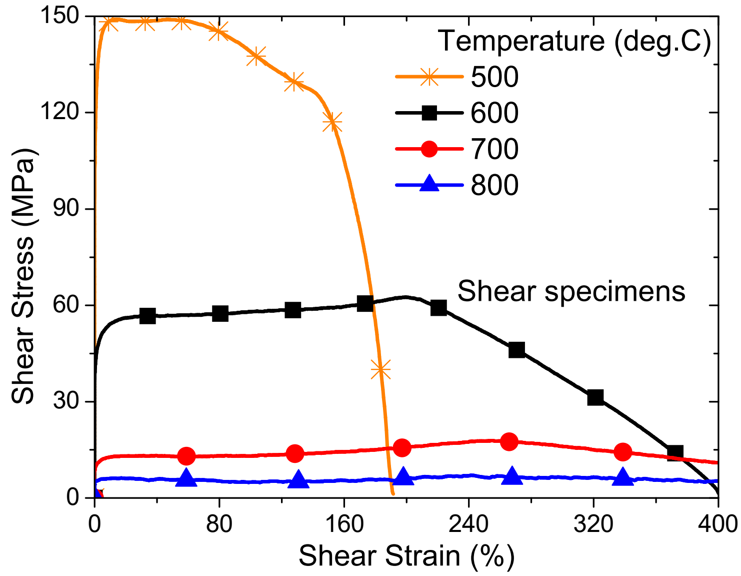

(b)

Figure 9. Comparison of shear stress-strain curve of Zr-2.5% Nb for shear loading at different temperatures (a) upto 500˚C (b) 500–800˚C.

Table 5. Summary of mechanical properties of Zr-2.5Nb alloy for shear loading.

Temperature (˚C)	Avg. Yield strength (MPa)	Avg. Ultimate tensile strength (MPa)	Avg. Ductility (%)
RT (25)	300	396	40
100	264	324	60
200	216	288	84
300	198	270	115
400	174	216	150
500	114	150	190
600	42	62.4	400
700	12	18	750
800	5.4	6.84	760

4. Comparison of Engineering Stress-Strain Curves of Zr2.5Nb Alloy for Different Orientations at Different Temperatures

During fabrication of pressure tube, extrusion and pilgering takes place that develops a strong texture leading to anisotropic mechanical properties. This texturing is beneficial as it helps in mitigating the formation of radial hydrides during the operational life of the pressure tubes. Hence, it has been seen that the material properties of pressure tube are functions of orientation distribution of the grains along the three perpendicular directions of the tube i.e., transverse, longitudinal and radial directions.

The effect of orientation of the specimen on engineering stress-strain curve is shown in **Figure 10** for different test temperatures. It can be observed from Figure 10 that the stress-strain curve of the pressure tube material is highly anisotropic in nature. It can be seen that the yield strength and ultimate tensile strength is highest in transverse direction followed by longitudinal and radial

 doi:10.20944/preprints202604.0659.v1

directions. This is due to the alignment of basal poles along the transverse direction during fabrication of pressure tubes.

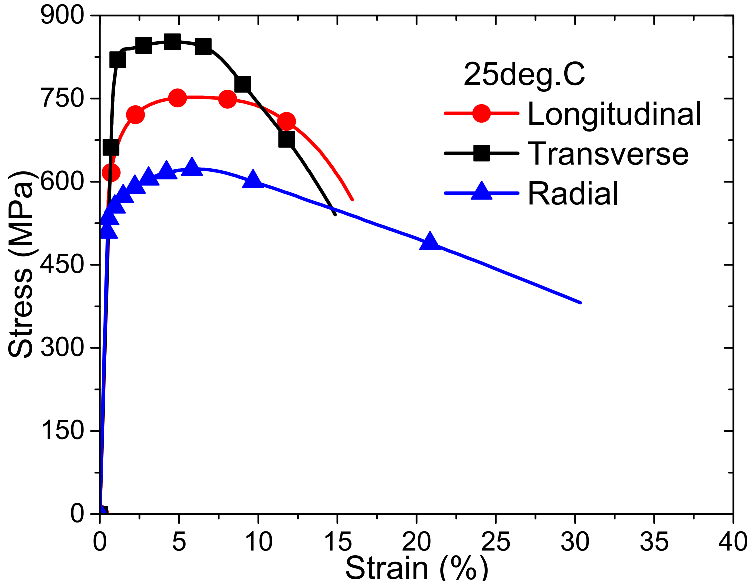

(a)

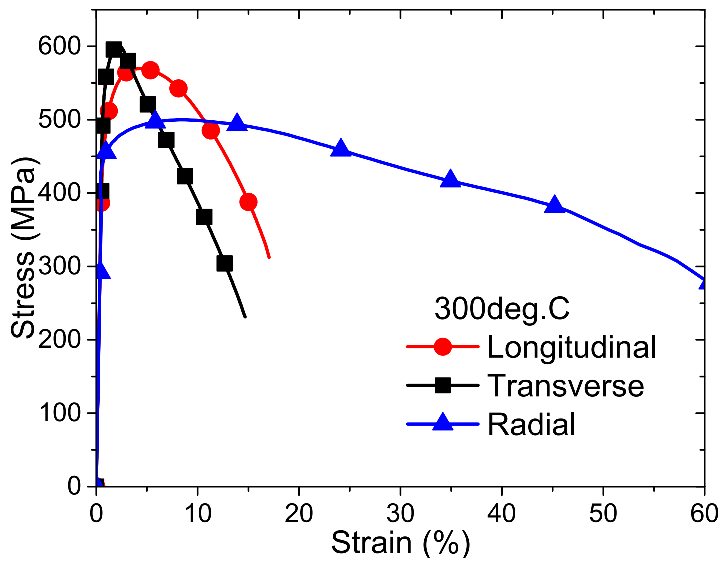

(b)

 doi:10.20944/preprints202604.0659.v1

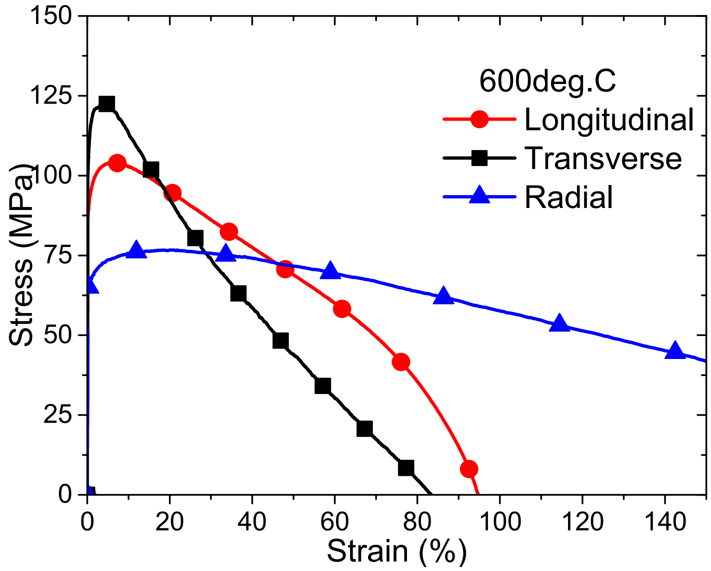

(c)

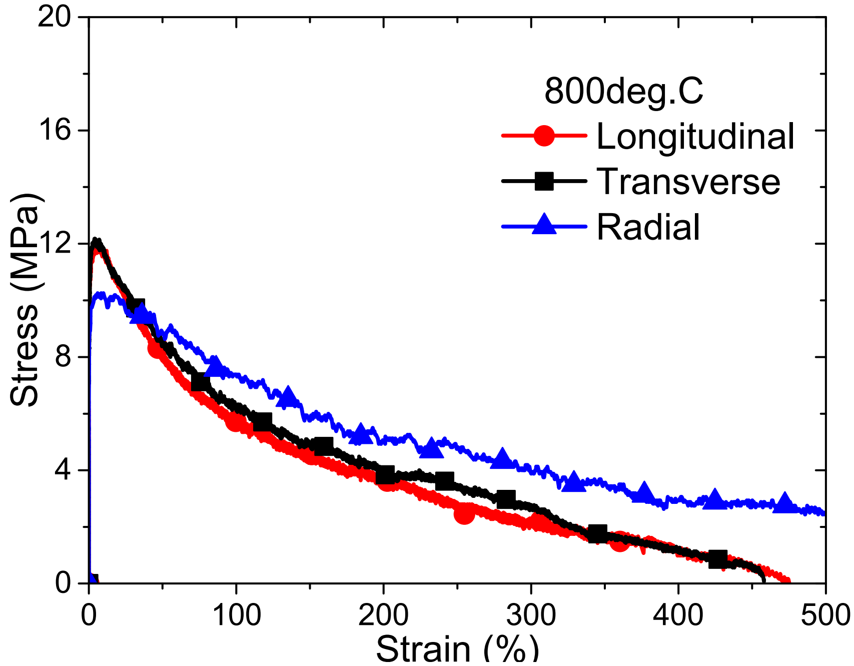

(d)

Figure 10. Comparison of engineering stress-strain curves of Zr-2.5% Nb material for different specimen orientations and at various temperature conditions. Data for (a) 25°C; (b) 300°C; (c) 600°C, (d) 800°C.

The ductility in radial direction is highest followed by the longitudinal and transverse directions. Ductility of the radial specimen gets increased up to 700% with the increase in temperature to 800°C. It can also be observed that the hardening (quantified as the ratio of UTS to YS) is highest in case of longitudinal specimen as compared to the other specimen orientations. It is observed that there is rapid reduction in strength of transverse specimen after UTS is reached. It is seen that the anisotropy gets reduced with the increase in temperature from 25 to 800°C. The strength of transverse and longitudinal specimen becomes identical as the temperature is increased to 800°C.

5. Evaluation of Anisotropic Factors of Generalized Hill's Yield Function

Hill's quadratic yield criteria has been used to determine the PT deformation with anisotropy. The quadratic yield criterion has the following form.

$$F\left(\sigma_{11}-\sigma_{22}\right)^2+G\left(\sigma_{22}-\sigma_{33}\right)^2+H\left(\sigma_{33}-\sigma_{11}\right)^2+2L\sigma_{12}^2+2M\sigma_{23}^2+2N\sigma_{31}^2=\sigma_{\mathbf{eq}}^2 \quad (1)$$

where *F, G, H, L, M, N* are anisotropic factors that have to be determined experimentally, σ_{ij} are the stress components as shown in Figure 22 and $\sigma_{\mathbf{eq}}$ is the equivalent stress for yielding of material in tension. The factors can be evaluated from the stress components and the equivalent stress using Eqs. (2-5) respectively.

$$F=\frac{{\sigma_{\text{eq}}}^2}{2}\left(\frac{1}{\left(\sigma_{22}^y\right)^2}+\frac{1}{\left(\sigma_{33}^y\right)^2}-\frac{1}{\left(\sigma_{11}^y\right)^2}\right) \quad (2)$$

$$G=\frac{{\sigma_{\text{eq}}}^2}{2}\left(\frac{1}{\left(\sigma_{33}^y\right)^2}+\frac{1}{\left(\sigma_{11}^y\right)^2}-\frac{1}{\left(\sigma_{22}^y\right)^2}\right) \quad (3)$$

$$H=\frac{{\sigma_{\text{eq}}}^2}{2}\left(\frac{1}{\left(\sigma_{11}^y\right)^2}+\frac{1}{\left(\sigma_{22}^y\right)^2}-\frac{1}{\left(\sigma_{33}^y\right)^2}\right) \quad (4)$$

$$L=\frac{3}{2}\frac{\tau_{\text{eq}}^2}{\left(\sigma_{23}^y\right)^2} \quad (5)$$

In Eq. (5), τ_{eq} is are the equivalent stresses for shear yielding of material. The relation between σ_{eq} and τ_{eq} is given by $\tau_{\text{eq}}=\frac{\sigma_{\text{eq}}}{\sqrt{3}}$. Four equations i.e., Eq. (2) to Eq. (5) are solved simultaneously to evaluate the four unknown anisotropic factor F, G, H and L. Here σ_{11}, σ_{22} and σ_{33} are the normal stresses in transverse, longitudinal and radial directions of the pressure tube respectively as shown in **Figure 11**.

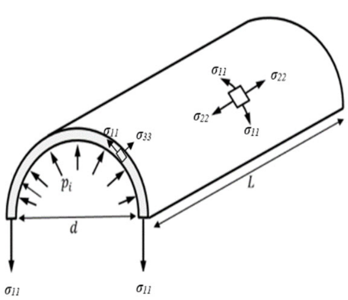

Figure 11. Representation of stress components in pressure tube (1 being transverse, 2 being longitudinal and 3 being radial orientations).

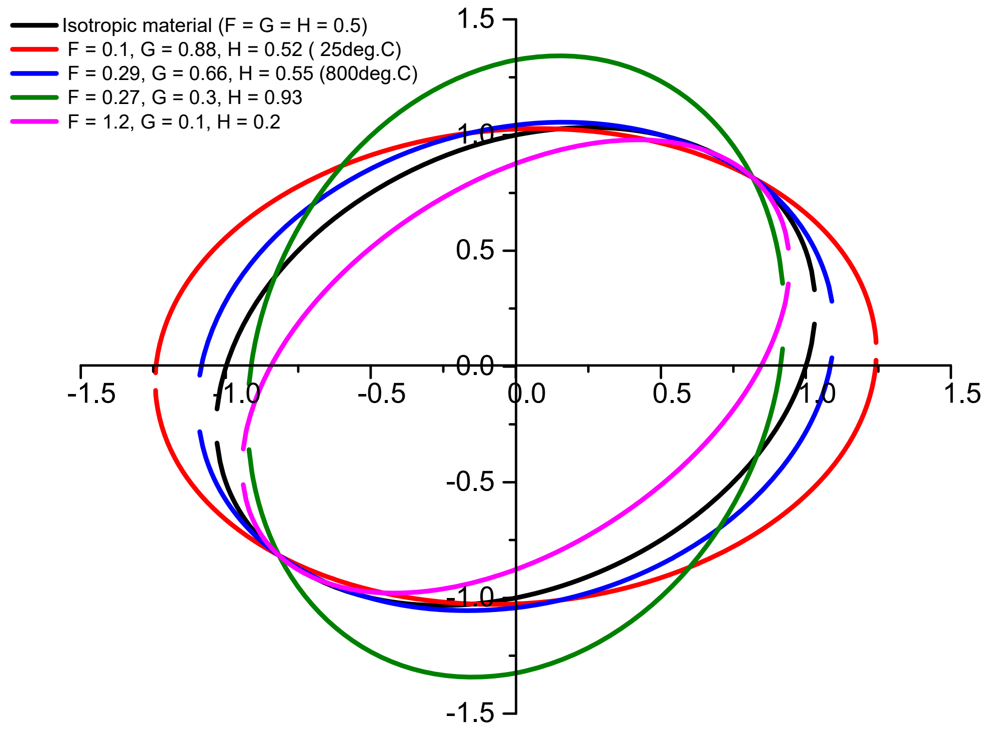

Figure 12. Comparison of Hill's anisotropic yield surface with different combinations of F, G and H parameters.

With the change in anisotropic parameters i.e., F, G and H, there will be simultaneous change in shape and orientation of the yield surface of material as shown in **Figure 12**. It can be observed from Figure 12 that, when the value of 'G' is large compared to 'F' and 'H', yield curve elongates towards the x-axis (transverse direction of pressure tube). Similarly, if the value of parameter 'H' is large as compared to other factors, yield surface will elongate towards y-axis. Combination of the above two cases is observed when the value of 'F' is large compared to 'G' and 'H'. There will be shrinking of the yield stress curve near to 45° axis and a corresponding decrease in the yield stress is observed in both 1 (transverse) and 2 (longitudinal) orientations. The change in yield surface with change in temperature is also shown in Figure 12. It can be seen that with the increase in temperature to 800 °C, the yield surface shift towards isotropic case.

An algorithm has been utilized to determine the values of anisotropic factor by solving the simultaneous equations, i.e., Eqs. (2-5). True stress-strain data obtained from the experiment has been used for determination of anisotropic parameters. The value of anisotropic factors changes with the temperature and equivalent plastic strain values. The variation of the anisotropic parameter 'G' with the increase in equivalent plastic strain is shown in **Figure 13(a)**. An exponential decrease in the value of parameter 'G' with the increase in equivalent plastic strain is observed from Figure 13(a). After certain value of plastic strain, the values of anisotropic factors gets converged to a constant value that indicated the saturation in strain hardening of the material. Similar exponential decrement nature of variation is observed for all the anisotropic factors (i.e., F, G, H, L) with respect to plastic strain. Accordingly, an exponential equation has been used to express the variation of the anisotropic factors with respect to the equivalent plastic strain for different temperatures. Eq. (6) shows the form of the equation, where 'y' represents the anisotropic factor, 'x' represents the equivalent plastic strain, y_0, A_1 and t_1 are the constants of the exponential form. Figure 13(a) shows the functional form of the parameter G at room temperature w.r.t. equivalent plastic strain and its comparison with actual data from experiment. The constants for all the anisotropic factors (i.e., F, G, H, L) as functions of temperature are shown in **Table 6**.

 doi:10.20944/preprints202604.0659.v1

$$y = y_0 + A_1 e^{-x/t_1} \quad (6)$$

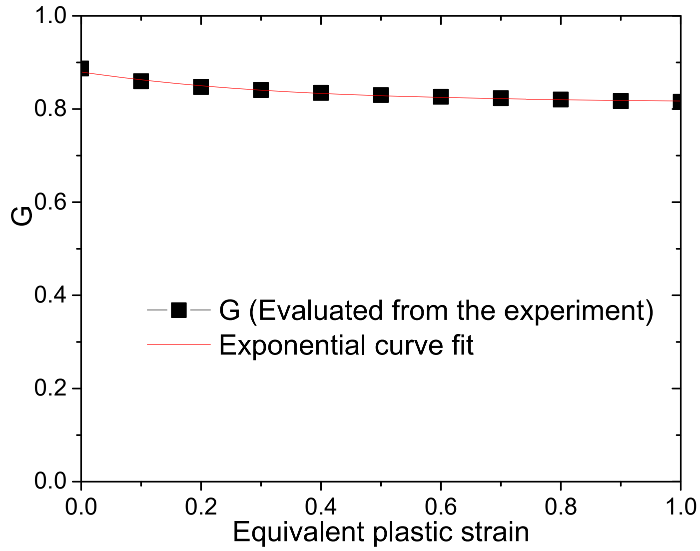

(a)

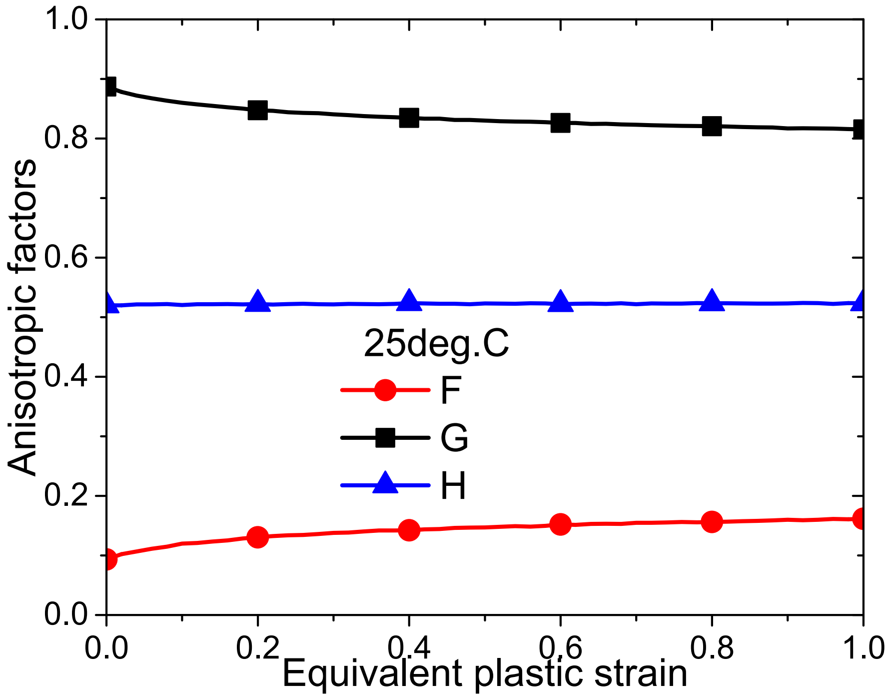

(b)

 doi:10.20944/preprints202604.0659.v1

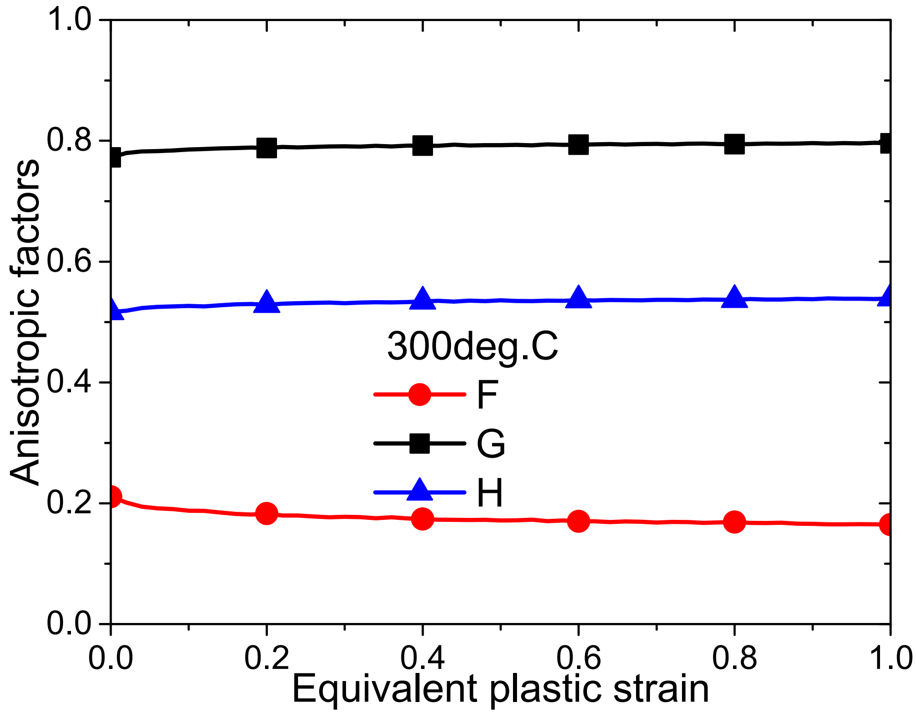

(c)

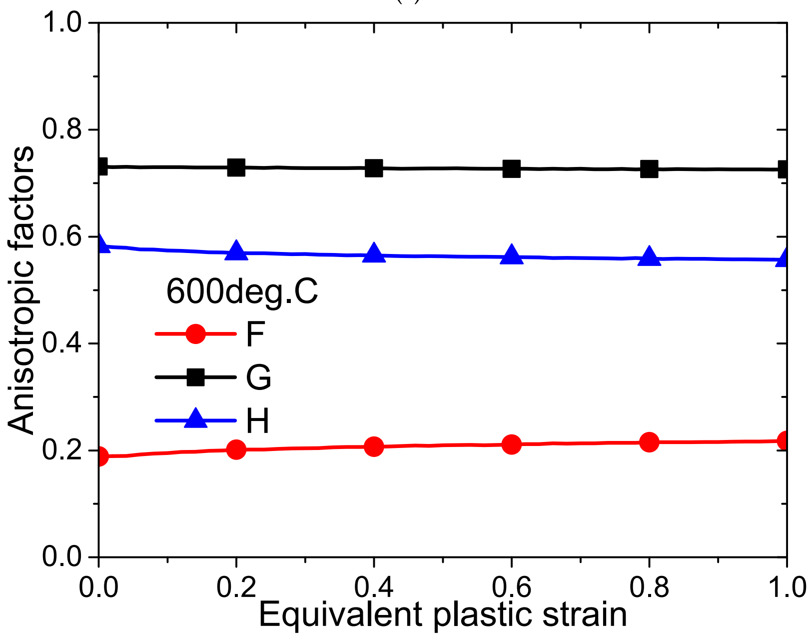

(d)

Preprints.org (www.preprints.org) | NOT PEER-REVIEWED | Posted: 9 April 2026 doi:10.20944/preprints202604.0659.v1

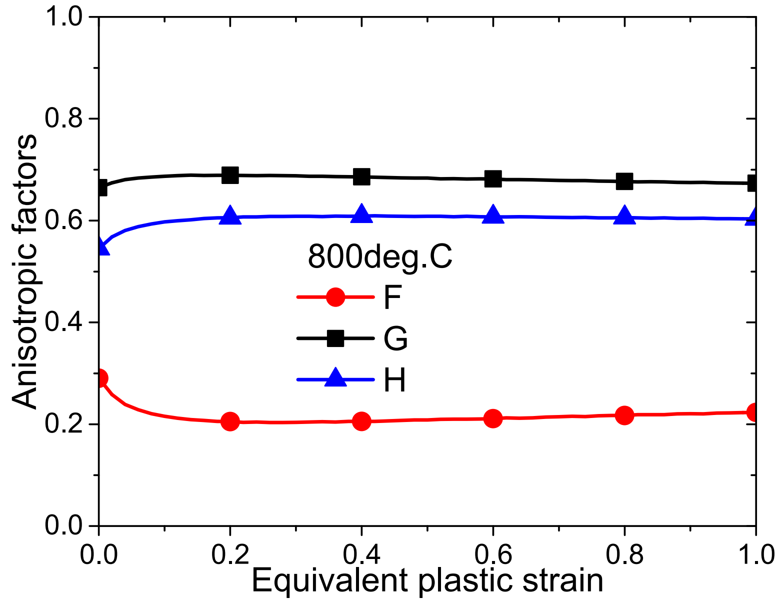

(e)

Figure 13. (a) Variation of anisotropic factor 'G' with equivalent plastic strain at room temperature and its functional representation. Variation of anisotropic factors (F, G and H) with equivalent plastic strain at different temperatures, i.e., Data at (b) 25°C (room temperature); (c) 300˚C; (d) 600˚C; (e) 800˚C.

Table 6. Values constants for evaluation of anisotropic factors of Hill's model.

Temperature (˚C)	Constants of functional form	F	G	H	L
RT (25)	y_0	0.163	0.814	0.523	2.445
	A_1	-0.063	0.065	-0.003	-0.205
	t_1	0.336	0.333	0.268	0.303
100	y_0	0.0864	0.829	0.585	2.317
	A_1	0.0273	-0.009	-0.019	-0.106
	t_1	0.0917	0.0203	0.178	0.359
200	y_0	0.0726	0.791	0.635	2.22
	A_1	0.0677	0.0145	-0.0758	-0.053
	t_1	0.179	0.621	0.243	0.59
300	y_0	0.166	0.795	0.538	2.12
	A_1	0.0366	-0.0179	-0.0189	0.002
	t_1	0.241	0.2114	0.269	0.001
400	y_0	0.174	0.742	0.581	1.98
	A_1	-0.0016	0.0197	-0.015	0.057
	t_1	0.22	0.416	0.165	0.0943
500	y_0	0.24	0.712	0.542	1.87
	A_1	-0.0126	0.099	-0.014	0.0078
	t_1	0.275	0.312	0.229	0.083
600	y_0	0.22	0.724	0.556	1.616
	A_1	-0.0313	0.007	0.0248	0.149

 doi:10.20944/preprints202604.0659.v1

	t_1	0.457	0.75	0.374	0.227
700	y_0	0.294	0.717	0.54	1.405
	A_1	-0.111	-0.0219	-0.004	0.249
	t_1	0.649	0.021	0.0578	0.43
800	y_0	.212	0.682	0.606	1.362
	A_1	0.079	-0.017	-0.0606	0.196
	t_1	0.0346	0.0169	0.049	0.0357

Figure 13 shows the variation of anisotropic factors (F, G and H) with the increase in equivalent plastic strain at room temperature. It is observed that the anisotropic factors converge to a constant value after some value of equivalent plastic strain. Value of parameter 'G' is the highest as compared to other factors indicating the maximum yield strength along the transverse orientation of the pressure tube. Values of parameters F, G and H at the initial yield at room temperature are 0.093, 0.887 and 0.519 respectively.

Similar observation has been made related to the variation in anisotropic factors for the tests carried out at different temperature upto 800°C as shown in Figure 13. The values of parameters F, G and H at the initial yield are 0.211, 0.772 and 0.516 respectively at 300°C and 0.189, 0.731 and 0.583 respectively at 600°C. The corresponding values are 0.290, 0.665 and 0.545 respectively when the temperature is increased to 800°C. The values of the anisotropic factors evaluated at the yield strain are listed in **Table 7**.

It can be observed from **Figure 14** that with the increase in temperature, the values of parameter 'G' at the yield surface reduces. It reduces from 0.88 at room temperature to 0.66 at 800˚C. Also, this value gets constant after the specimen has undergone some equivalent plastic strain. The value of 'F' parameter lies in the range of 0.1 to 0.3. No specific trend is observed in the value of F due to increase in temperature from room temperature to 800˚C. Value of H lies in a small range of 0.51 to 0.58.

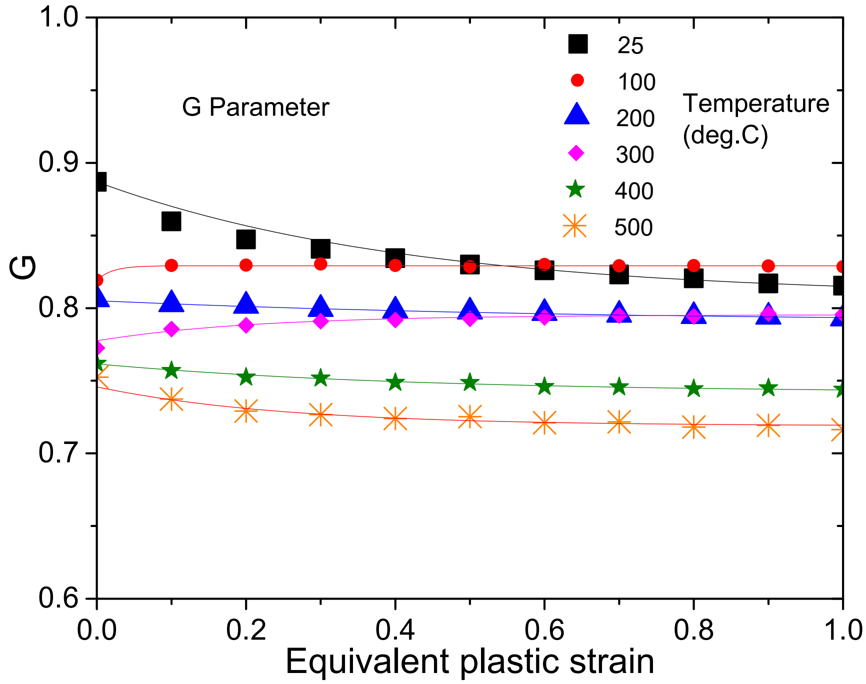

(a)

Preprints.org (www.preprints.org) | NOT PEER-REVIEWED | Posted: 9 April 2026 doi:10.20944/preprints202604.0659.v1

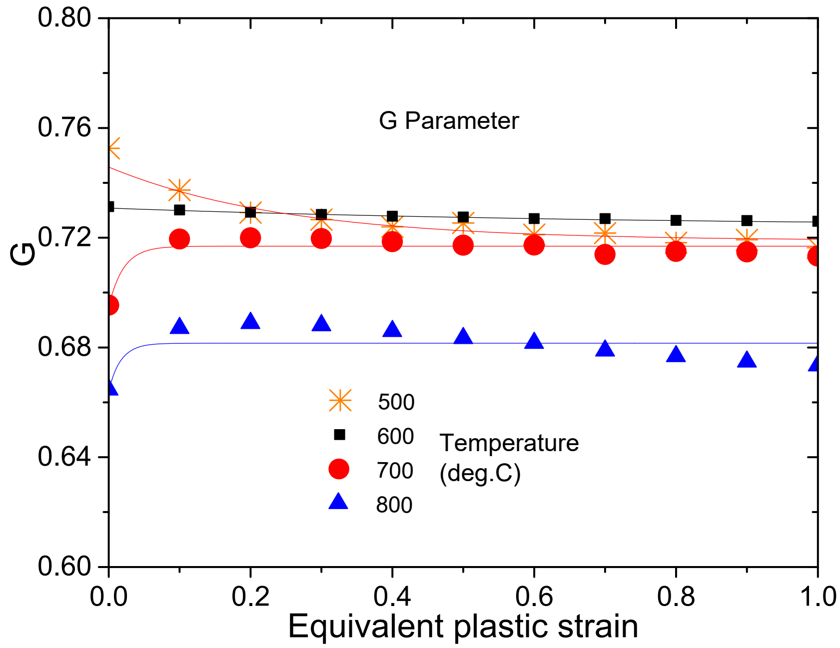

(b)

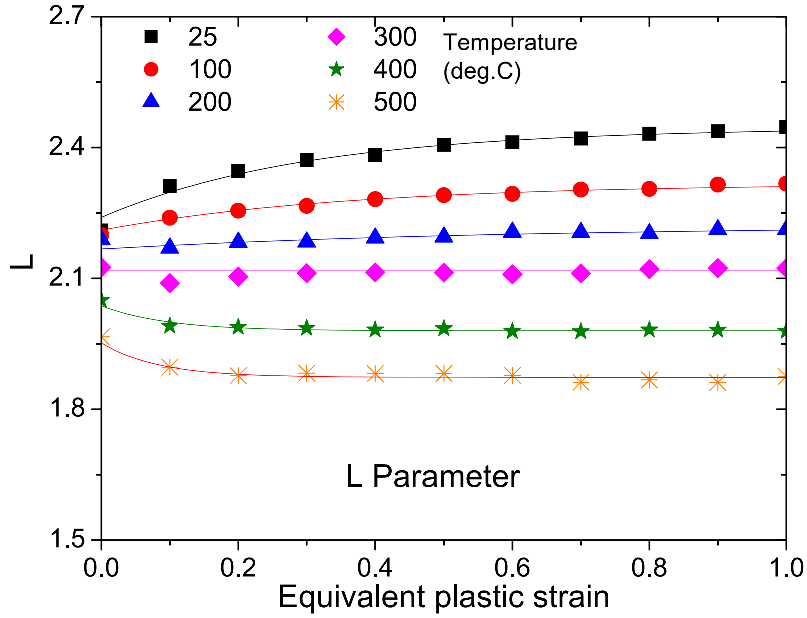

(c)

Preprints.org (www.preprints.org) | NOT PEER-REVIEWED | Posted: 9 April 2026 doi:10.20944/preprints202604.0659.v1

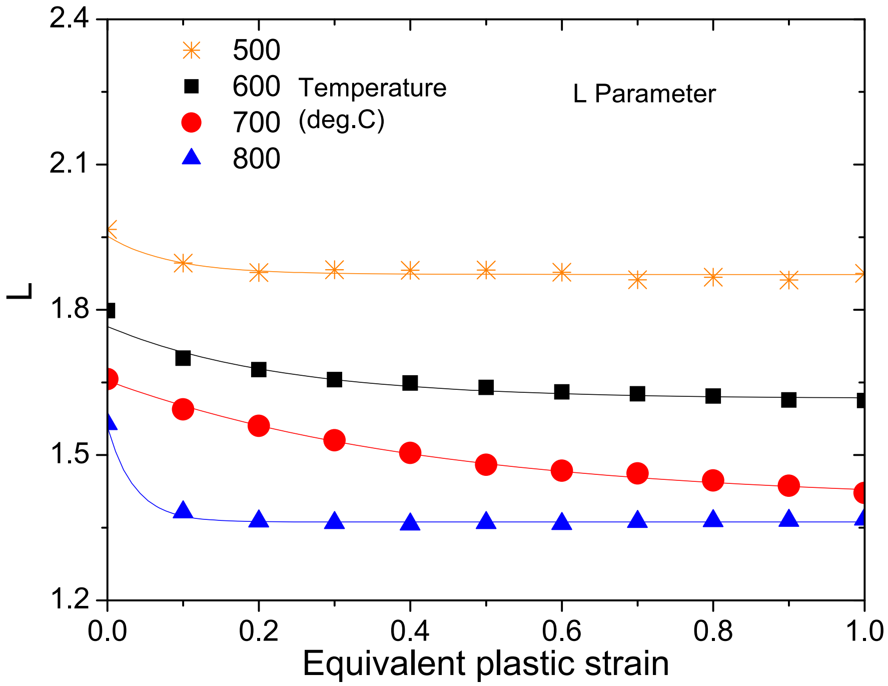

(d)

Figure 14. Variation of anisotropic factor (G) with strain for different temperatures (a) upto 500˚C (b) 500–800˚C. Variation of anisotropic factor (L) with strain for different temperatures (c) upto 500˚C (d) 500–800˚C.

Table 7. Summary of the anisotropic factors at initial yield for different temperatures.

Temperature (˚C)	F	G	H	L
RT (25)	0.093	0.887	0.519	2.21
100	0.119	0.819	0.561	2.19
200	0.157	0.806	0.544	2.18
300	0.211	0.772	0.516	2.125
400	0.175	0.762	0.563	2.005
500	0.224	0.752	0.524	1.966
600	0.189	0.731	0.583	1.798
700	0.189	0.695	0.534	1.657
800	0.290	0.665	0.545	1.564

With the increase in temperature, value of H tends to increase while there is simultaneous reduction in value of G parameter. This indicates that there is reduction between the values of G and H parameter with the increase in temperature. Hence, it can be inferred that there shall be convergence between the values of strength in longitudinal and transverse specimen with the increase in temperature as shown in **Figure 14(a, b)**. It can be concluded that there is reduction in anisotropy observed in the pressure tube material with the increase in temperature above 600˚C. Similar trend has been observed from the experimental results discussed in previous sections.

Variation of shear anisotropic factor 'L' with temperature is shown in **Figure 14(c, d).** The parameter 'L' increases with the increase in equivalent plastic strain and reaches a constant value after some equivalent plastic strain. The value of shear anisotropic factor L at initial yield has been evaluated as 2.21, 2.125, 1.798, and 1.564 for tests carried out at RT, 300°C, 600°C and 800°C respectively. It can be observed that the value of parameter 'L' decreases with the increase in temperature. Also, value of 'L' reaches near to 1.5 value at temperature of 800°C indicating that the material is near to isotropic in nature. Hence, the anisotropy in pressure tube material decreases as the temperature reaches 800°C.

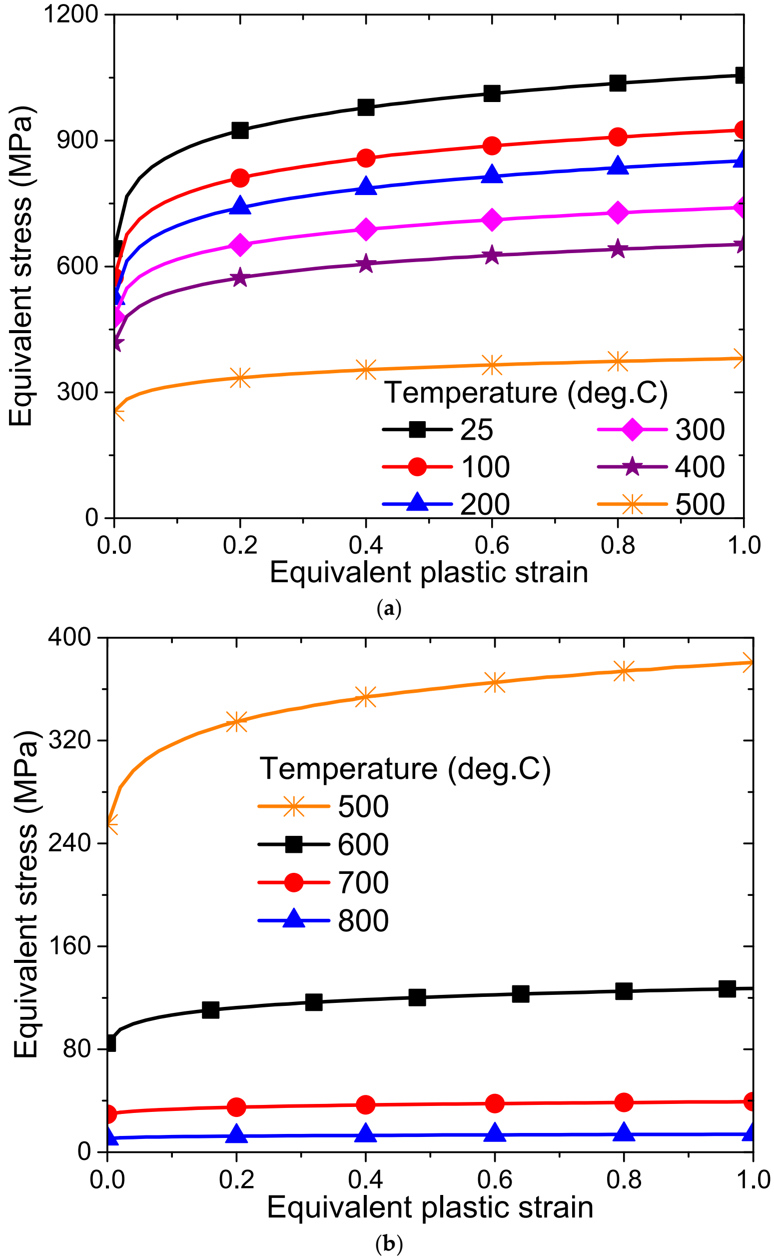

Figure 15. Variation of effective stress-strain curve of the material at different temperatures (a) upto 500˚C (b) 500–800˚C.

Figure 15 shows the comparison of effective stress-strain curves as a function of temperature. It can be observed that the equivalent YS and UTS get reduced with the increase in temperature. The effective yield strength of the pressure tube material has been evaluated as 642, 480, 85 and 10.6 MPa respectively at RT, 300°C, 600°C and 800°C respectively. These data can be used for elastic-plastic stress analysis of pressure tube components of nuclear reactors for design and safety analysis.

 doi:10.20944/preprints202604.0659.v1

6. Conclusions

Tensile tests have been carried out using the specimens cut from quadruple melted Zr2.5Nb pressure tube of 550 MW PHWR along longitudinal, transverse and radial directions in the temperature range of 25 to 800^{o}C. Shear properties have also been evaluated at the above temperatures by using the specimen machined from longitudinal-transverse plane. An algorithm has been developed to determine the anisotropic parameters i.e., F, G, H and L of Hill's yield function as a function of temperature and equivalent plastic strain using the experimental data.

Following conclusions can be drawn from the experiments:

- Transverse direction specimen has highest strength (YS and UTS) while radial specimen has the lowest strength as compared to other direction specimens at all temperature values.
- Ductility of the specimen is the highest for the radial specimen followed by longitudinal and transverse orientation. With the increase in temperature above 600^{o}C, material undergoes superplastic deformation with strain values reaches above 400% at 800^{o}C.
- Values of the anisotropic factors (i.e., F, G, H and L) at the yield strain have been evaluated as 00.093, 0.887, 0.519 and 2.21 respectively at room temperature. Similar values at 300^{o}C are 0.211, 0.772, 0.516 and 2.125. These values are 0.189, 0.731, 0.583 and 1.798 respectively at 600^{o}C and 0.290, 0.665, 0.545 and 1.564 respectively at 800^{o}C.
- Higher strength in the transverse direction occurs due to largest value of anisotropic parameter 'G' as compared to other factor (i.e., F and H). This indicated the shifting of the yield surface towards transverse direction.
- Value of anisotropic factor G reduces from 0.88 to 0.66 with the increase in temperature from 25 to 800^{o}C. Also, value of parameter 'L' converges near to the isotropic value (1.5) as the temperature is increased to 800^{o}C. This indicates that with the increase in temperature, anisotropy in pressure tube material decreases.
- Anisotropic parameters changes with material flow and hence, these are functions of equivalent plastic strain. It has been observed that the anisotropic factors (i.e., F, G, H and L) follow exponential variation with respect to equivalent plastic strain. These parameters reach a constant value after some value of plastic strain accumulation. The constants of the functional forms of all the parameters have been determined for temperatures upto 800^{o}C.

Author Contributions: For research articles with several authors, a short paragraph specifying their individual contributions must be provided. The following statements should be used "Conceptualization, MKS; methodology, AS and MKS; software, AS and MKS.; validation, AS and MKS.; formal analysis, AS and MKS investigation, AS and MKS; resources, MKS; data curation, AS and MKS; writing—original draft preparation, AS and MKS; writing—review and editing, MKS; visualization, AS and MKS; supervision, MKS; project administration, MKS; funding acquisition, N.A. All authors have read and agreed to the published version of the manuscript." Please turn to the CRediT taxonomy for the term explanation. Authorship must be limited to those who have contributed substantially to the work reported.

Funding: This research received no external funding.

Institutional Review Board Statement: N.A.

Informed Consent Statement: N.A.

Data Availability Statement: Data shall be made available on request and shall be uploaded to https://www.mdpi.com/article/doi/s1.

Acknowledgments: N.A.

Conflicts of Interest: The authors declare no conflicts of interest.

References

1. R.A. Holt, In-reactor deformation of cold-worked Zr–2.5Nb pressure tubes, Journal of Nuclear Materials, 372 (2-3), 2008, pp. 182-214.
2. Tianshuo Song, Shuguang Liu, Bohan Chen, Ziyao Cui, Xianrui Zou, Shiliang Zhang, Qiang Li, Chaoqun Xia, Enhanced corrosion and wear resistance via thermal oxidation treatment on Zr-2.5Nb alloy for implant applications, Surface and Coatings Technology, 458, 2023, 129365.
3. Chaoqun Xia, Qianying Liu, Tianshuo Song, Bohan Chen, Shuguang Liu, Qiang Li, Corrosion behavior and wear resistance of Zr-2.5Nb alloy after thermal oxy-nitriding treatment, Surface and Coatings Technology, Volume 446, 2022, 128756.
4. Remigijus Janulionis, Gintautas Dundulis, Study of the impact of hydrides on the fracture toughness of Zr-2.5Nb alloy, Nuclear Engineering and Design, 416, 2024, 112803.
5. Y. Idrees, Z. Yao, J. Cui, G.K. Shek, M.R. Daymond, Zirconium hydrides and Fe redistribution in Zr-2.5%Nb alloy under ion irradiation, Journal of Nuclear Materials, 480, 2016, pp.332-343.
6. Chunting Pan, Guannan Zhao, Yichen Bao, Zhiming Zhang, Xiuqiang Shi, Fanjiang Meng, Jianqiu Wang, Hongliang Ming, Effect of temperature on the delayed hydride cracking rate of Zr-2.5Nb alloy pressure tubes, Journal of Nuclear Materials, 588,2024,154778.
7. Guannan Zhao, Peng Zhang, Long Zhang, Qinwen Luo, Qiang Yu, Shitong Xu, Lijuan Hu, Guanze He, Hongchang Wang, Meiyi Yao, Preparation and Performance of Pre-oxidation Films on Zr-2.5Nb Alloy Pressure Tubes for Heavy Water Reactors, Corrosion Science,2026, 113808.
8. S. Dutta, P.S. Robi, P. Majumdar, High temperature tensile properties of Zr-2.5 wt%Nb alloy pressure tubes used in IPHWR220, AIP Conference Proceedings 2284 (2020) 020002.
9. Cheng Liu and Douglas Scarth, Validation and refinement of statistical-based fatigue crack initiation model for axial flaws in Zr-Nb pressure tubes, Proceedings of the ASME 2023 Pressure Vessels & Piping Conference PVP2023, July 16-21, 2023, Atlanta, Georgia, PVP2023-106363.
10. R.O. Oviasuyi, R.J. Klassen, Assessment of the anisotropic flow stress and plastic strain of Zr–2.5%Nb pressure tubes at temperature from 25 °C to 300 °C, Journal of Nuclear Materials, 429 (1-3), 2012, pp. 7-12.
11. M.K. Samal, A. Syed, D. Sen, J. Chattopadhyay, Experimental evaluation of orientation and temperature dependent material stress-strain curves of Zr2.5%Nb Indian pressure tube material and development of a suitable anisotropic material model, Journal of Nuclear Materials, 530, 2020, 151970.
12. N. Christodoulou, C.N. Tomé, Anisotropy of plastic flow in Zr-2.5Nb pressure tube material analysed using a viscoplastic self-consistent approach, Acta Materialia, 283, 2025, 120503.
13. Huilong Yang, Anisotropic effects of radiation-induced hardening in nuclear structural materials: A review, Journal of Nuclear Materials, 561, 2022, 153571.
14. Xikai Xu, Wenjing Ding, Chen Bao, Yupeng Cao, Guannan Zhao, Yield anisotropy and failure behavior of domestic Zr-2.5Nb pressure tubes: A study combining microstructure and the Hill'48 criterion, European Journal of Mechanics—A/Solids, 117, 2026, 105990,
15. P. Hovington, P.T. Pinard, M. Lagacé, L. Rodrigue, R. Gauvin, M.L. Trudeau, Towards a more comprehensive microstructural analysis of Zr–2.5Nb pressure tubing using image analysis and electron backscattered diffraction (EBSD), Journal of Nuclear Materials, 393 (1), 2009, pp. 162-174.
16. Dong-Hyun Ahn, Sangyeob Lim, Gyeong-Geun Lee, Young-Bum Chun, Study on the mechanical properties and microstructure of Zr-2.5wt%Nb pressure tube material, Journal of Nuclear Materials, 523, 2019, pp. 458-471.
17. Qianqian Luo, Jianming Yin, Fuzhou Han, Wenzheng Xu, Bo Gao, Longgang Tong, Intermediate heat treatment effects on the hot-rolled Zr-2.5Nb alloy: Microstructure and mechanical properties, Journal of Alloys and Compounds, 1051, 2026, 185988.
18. Mengyao Tian, Bo Li, Guocheng Sun, Da Wu, Cong Li, Yimin Gao, Chenyu Liang, Microstructure characterization and dynamic recrystallization behavior analysis in hot rolling of biomedical Zr-2.5Nb alloy, Journal of Alloys and Compounds, 1057, 2026, 186951.
19. M.G. Isaenkova, A.V. Tenishev, O.A. Krymskaya, S.D. Stolbov, V.V. Mikhal'chik, V.A. Fesenko, K.E. Klyukova, Influence of the structural state and crystallographic texture of Zr-2.5% Nb alloy samples on the anisotropy of their thermal expansion, Nuclear Materials and Energy, 29, 2021, 101071.

 doi:10.20944/preprints202604.0659.v1

20. B.W. Williams, S. St Lawrence, B.W. Leitch, Comparison of the measured and predicted crack propagation behaviour of Zr–2.5Nb pressure tube material, Engineering Fracture Mechanics, 78 (18), 2011, pp. 3135-3152.
21. Shengjia Wu, Jwo Pan, Douglas A. Scarth, Finite element analyses of crack extensions in curved compact tension specimens of irradiated Zr-2.5Nb pressure tube materials by nodal release method and cohesive zone modeling approach, Engineering Fracture Mechanics, 271, 2022, 108676.
22. Xikai Xu, Zhiyi Wu, Chen Bao, Yupeng Cao, Guannan Zhao, Investigation of the tensile fracture behavior and failure criteria of domestic Zr-2.5Nb alloy under different stress triaxiality conditions, Engineering Fracture Mechanics, 318, 2025, 110991.
23. Vaclav Sklenicka, Kveta Kucharova, Petr Kral, Jiri Dvorak, Marie Kvapilova, Vera Vrtilková, Jakub Krejcí, Investigation of the thermal creep behaviour of non-irradiated Zr1%Nb cladding alloys between 623 and 1223K, Journal of Nuclear Materials, 583, 2023, 154518.
24. Vaclav Sklenicka, Kveta Kucharova, Petr Kral, Jiri Dvorak, Marie Kvapilova, Vera Vrtilkova, Jakub Krejci, Thermal creep in a pre-hydrided Zr1% Nb nuclear fuel cladding tube, Journal of Nuclear Materials, 596, 2024, 155084.